SHOCK-WAVE PROPAGATION THROUGH A VERTICAL FOAM COLUMN WITH A DENSITY GRADIENT

A. B. Britan, I. N. Zinovik, and V. A. Levin

UDC 532.552.529.5

Foamy agents are widely used in blast welding [1], fire fighting [2], and coal mining [3]. Because of the large volumes involved, foam used for protection often contains inhomogeneities, gaps, and plugs which affect its mechanical and physical characteristics. Thus, in the case of explosion protection, the wave interaction, the motion of the shock-wave (SW), and the pressure impulse on the protected structures can significantly vary within the foam. It has been found [4-7] that the SW dynamics and profile in foam depend on the SW velocity V_f and the length of the compression phase. When the speed of sound in the foam-filling gas $a_0 > V_f$, the SW develops a forerunner with a wide relaxation zone and a pressure increase to equilibrium. If $a_0 < V_f$, no forerunner is produced. Experiments with shock tubes have usually been limited to $V_f < 1$ km/sec, with a mean foam density ρ_0 ranging from 5 to 30 kg/m^3 [8, 9]. Vertical [10, 11] and horizontal [6-9] foam layers of varying thickness have been used, with foam filling the entire tube channel or part of it near the end wall [11]. Most reports give no details on the characteristics of the foaming solution, the disperse composition of the foam, or other variables which would make it possible to compare the results of different studies. Scant attention is given to structural changes across the foam layer, although it has been found [12] that the discharge of liquid from the foam (i.e., syneresis [13]) can affect the SW shape and characteristics.

The usual profile of an incoming wave is analogous to that behind explosion waves, i.e., it is approximately triangular [10]. An SW with an extended compression phase interacts differently with foam [6, 7], and it is therefore worth comparing the behavior of disturbances of different profiles in foam.

In this study we examined the propagation of SWs with different compression phases in foam. We used a vertical tube filled with bubbled foam undergoing appreciable syneresis. This simulates the conditions produced in actual tests of foam protection against SW impact [14].

1. Experimental Procedure. We used a vertical shock tube of polished Plexiglas with a channel length L = 1440 mm and inner diameter D = 52 mm. The high-pressure chamber was made of stainless-steel tube sections of the same diameter and length ℓ = 40 and 800 mm. Mounted on the channel walls and tube end were miniature 800 kHz pressure pickups (a total of 10). The pickup signals were fed through a transponder to S8-17 oscillographs. The intervals between triggering pulses were measured with frequency meters within 0.1 μsec, and were used to determine the SW velocity V in air. A diaphragm composed of several layers of 20-μm dacron film was used in control the burst pressure p_4. The reproducibility of the SW velocity and the pickup signal amplitude was 1.5%. The velocity measurement error was ≤1%.

The foam was produced by bubbling air at $0.3 \cdot 10^5$ Pa overpressure through a porous filter and a layer of a 3% solution of PO-6K surfactant in water. The channel wall had a 5 mm hole 30 mm above the tube end, and the foam flowed in through a 400 mm rubber line of the same diameter as the hole. The rate of flow was 10.6 ml/sec, with a mean foam density $\rho_0 = 50 \pm 5$ kg/m^3. The position of the inlet hole prevented syneresis liquid from draining out of the channel; the liquid formed a thin layer ≈1 cm deep at the bottom. The density ρ_0 was determined by the control-volume method [13], which involves measuring the volume of liquid obtained by the complete breakdown of a foam column of given height h. The mean foam-bubble size, measured on photographs, was 400 μm to within 10%. The delay between the foam fill-up and firing time was in the range of 60 sec.

Moscow. Translated from Prikladnaya Mekhanika i Tekhnicheskaya Fizika, No. 2, pp. 27-32, March-April, 1992. Original article submitted July 4, 1990; revision submitted December 4, 1990.

 0021-8944/92/3302-0166$12.50

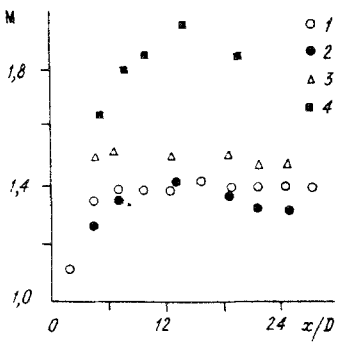

Fig. 1

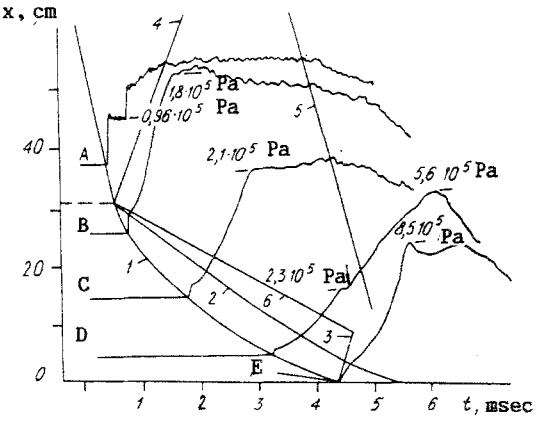

Fig. 2

2. Shock Tube Calibration. In an initial run of tests we measured the SW velocity and the pressure at various distances from the diaphragm. The tube channel was filled with air at atmospheric pressure, and the pressure in the chamber varied between 5 and $10 \cdot 10^5$ Pa. Given a total channel length of ≈30 diameters, approximately 1/3 of the tube had to be filled with foam in the main tests; the purpose of the calibration was therefore to ascertain the length of the region of constant SW velocity V and to characterize the flow at distances ≥20 diameters from the diaphragm.

Figure 1 shows the measured distribution of Mach numbers $M = V/a_0$ over the tube at thrust pressures of $5.6 \cdot 10^5$, $5.6 \cdot 10^5$ [sic], and $9.5 \cdot 10^5$ Pa (points 1-3). Points 4 are the experimental data of [15] for a pressure drop $p_4/p_0 = 5$ at the diaphragm and a reduced pressure in the channel. The data 1 and 3 were obtained with a long chamber (ℓ = 800 mm), and data 2 were obtained with a short chamber (ℓ = 4 cm).

We see from Fig. 1 that the length of the SW region does not exceed six diameters. The number M increases with p_4, and the variation of the experimental points is within 1.5% at a distance of ≥20 diameters from the diaphragm. In the short chamber experiments the expansion wave reflected from the chamber end overtakes the SW front, and a triangular wave with M = 1.3 is generated at ≈18 diameters from the diaphragm. On the basis of the calibration we choose the conditions of tests 1 and 2 for the foam experiments.

In contrast to our results, the data of [15] show the formation of an extended SW region (≈15 diameters). This is due to the fact that in [15] use is made of cellophane diaphragms which stretch considerably under load, producing a curved SW front in the impulse region. The front also arises more slolwy because the impulsive pressure in the channel is reduced. The distribution of M consequently shows a distinctive maximum at the far end of the SW region (points 4 in Fig. 1).

Some simple calculations based on [15, 16] indicate that the dacron diaphragms have a bursting time of 150 μsec or less, and the SW-region length is two to four diameters. The expansion wave overtakes the SW at a calculated distance of 13 diameters from the diaphragm. Also, the pressure-pickup oscillograms provide the means of characterizing the flow. In most of the tests with ℓ = 800 mm, the homogeneous state behind the incident SW lasts for 2 to 2.5 msec, and the signal-amplitude variation is less than 5%. Hence the SW velocity varies within $\sim \pm 3\% \cdot m^{-1}$ up the flow.

3. Analysis of Wave Diaphragm. In the tests we varied the form column height between 100 and 500 mm. The short columns are fairly homogeneous vertically, and made it possible to track the whole process from the SW arrival at the foam surface to the emergence of the SW reflected from the tube end. By means of a 300 mm column we studied the motion of the SW through foam with a nonuniform density produced by syneresis. Plotting the results on a space-time diagram yields a realistic wave pattern which cannot be obtained by other means, such as calculation by the pseudo gas model [5, 8] or other equilibrium foam models.

Figure 2 shows the wave pattern for a foam column of height h = 300 mm, SW velocity V = 470 m/sec, and chamber length ℓ = 800 mm. An extended-compression SW is reflected from the foam surface and is registered by pickup A. Pickups B-E, located in the foam, record the motion of the forerunner (curve 1); the peak pressure; the motion of the pressure peak

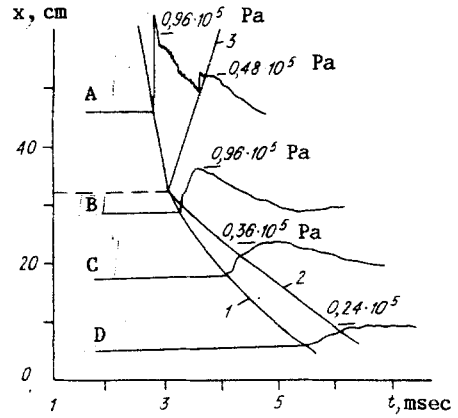

Fig. 3

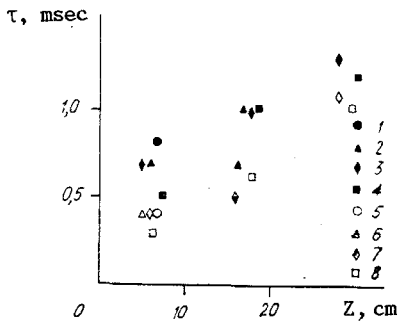

Fig. 4

(wavefront) at which the relaxation zone ends and equilibrium is approached behind the SW (curve 2); and the motion of the SW reflected from the end and from the foam surface (lines 3 and 4). The foam surface prior to the SW arrival is marked with a dashed line. The oscillograms of pickups A-C also show the arrival time of the expansion wave reflected from the chamber end (line 5) and the fulcutations produced by turbulence in the flow between the foam surface and the wave reflected by it. The fluctuations may be due to the SW crossing an irregular foam surface and a compression wave packet being reflected and reinforcing the reflected wave. A similar pressure rise behind the reflected wavefont appears in the oscillogram of pickup A. The onset of fluctuations in the oscillograms is associated with the arrival of the foam surface at the pickup and is used to plot its motion along the tube (line 6).

In the situation depicted in Fig. 2 the SW is reflected from the foam surface as a jump of similar size, while a transmitted wave with a well-defined forerunner compresses the foam column to about one-third its height. Compression ceases when the end-reflected wave returns to the foam surface. The point of return is above the level of pickup D, which is under foam all the time. The levels B-D clearly display the relaxation zone behind the forerunner front; the front velocity steadily decreases while its amplitude remains almost constant. The peak pressure at the edge of the relaxation zone steadily increases down the tube, and at pickup D it is nearly twice as high as at pickup B. The conditions behind the end-reflected wave are complicated by the relaxation zone. The forerunner reflected into the region of increasing pressure produces a pressure spike, which becomes flattened by interference from the foam surface and the arrival of the expansion wave from the chamber. The arrow in the oscillogram of pickup D indicates the arrival of a reflected wave with a fairly long pressure rise. The horizontal lines in the oscillogram denote the pressure.

Figure 3 shows some typical pressure oscillograms for the transmission of a triangular SW (chamber length ℓ = 40 mm, foam layer height h = 320 mm). As previously, pickup A registers the SW reflected from the foam surface, and the transmitted wave displays a forerunner and a relaxation zone in which the pressure rises up to $\approx 0.96 \cdot 10^5$ Pa near the foam surface. The forerunner velocity steadily decreases along the foam column, while its amplitude remains at about $0.3 \cdot 10^5$ Pa. We thus see that the forerunner characteristics are largely independent of the shape of the incoming SW.

The flow parameters behind the forerunner front are significantly affected by the air profile of the driving wave. Since the pressure steadily decreases in both the incident wave and the wave reflected from the foam surface, the peak pressure in the relaxation zone varies along with the driving pressure. The oscillograms of the foam-covered pickups do not show the amplitude fluctuations associated with gas turbulence. From the pattern of variation of the pressure we reconstructed the motion of the forerunner, of the pressure peak at the edge of the relaxation zone, and of the SW reflected by the foam surface (curves 1-3).

4. Discussion of Results. The available data on foams under normal conditions indicate that the phase interfaces in these complex polydisperse systems consist of film and channels [13]. The structural changes occurring during the transmission of a SW involve mainly the breakdown of the interfaces and the formation of drops [6-8]. The relaxation zone behind the forerunner front is produced by disintegration of the foam and by heating and accelera-

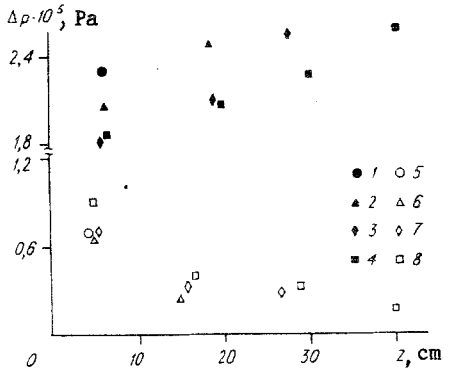

Fig. 5

tion of its particles to the gas velocity. Calculations show [6] that the efficiency of momentum and energy transfer in a gas suspension depends primarily on the inertia of the drops. The pressure profile in the relaxation zone thus represents the foam-particle dispersal dynamics [6].

Plotted in Fig. 4 are the relaxation times measured in experiments with foam columns of height h = 10.5 (points 1, 5), 20.5 (2, 6), 31.5 (3, 7), and 44.5 cm (4, 8). By using different column heights we could vary the distance Z covered by the SW between the foam surface and the measuring pickup. Points 1-4 were obtained with a long chamber (ℓ = 80 cm), and 5-8 with a short one (ℓ = 4 cm). The relaxation time increases with the distance Z in extended-compression waves and in triangular waves, though in the latter the relaxation ends sooner. The wave diagram in Fig. 2 shows that the equilibrium pressure at level D is nearly twice as high as at level B and that the SW velocity V_f (the equilibrium-pressure velocity) through the foam changes insignificantly. This behavior of the pressure and velocity stems from the nonuniform foam density over the column. As a result of syneresis, the upper foam layers in the channel dry out and the lower part of the tube fills up with liquid [13]. Using an "equivalent gas" approximation for the equilibrium foam parameters at the edge of the relaxation zone, we can write the Hugoniot function as

$$(p_1 - p_0)/p_0 = \Delta p/p_0 = 2\gamma(V^2/a^2 - 1)/(\gamma + 1),$$

where p_0 is the initial foam pressure in front of the SW; p_1 is the equilibrium pressure at the edge of the relaxation zone; γ is the effective adiabatic exponent of the equivalent gas; V_f is the velocity of the equilibrium-pressure region; $a = \sqrt{\gamma p_0/\rho}$ and ρ are the equilibrium speed of sound and the undisturbed foam density. The parameter γ depends on the mass content of liquid in the foam. In our case $\gamma \approx 1$ and p_0 = 1 atm, and hence the pressure at the edge of the relaxation zone $p_1 \approx V_f^2\rho$. We used this equation to calculate the densities at the measurement levels given in Fig. 2. The proportionality factor was V_f = 65 m/sec, as measured in that experiment. We found $\rho \approx$ 37, 68, and 114 kg/m^3 for levels B-D.

The measurement of the equilibrium pressure at the edge of the relaxation zone (Fig. 5) indicate that the SW effect on the foam varies with the profile and pressure of the incoming wave. In an extended-compression SW (the designation of the points in Fig. 5 is the same as in Fig. 4) the presssure increases with Z, which means that the foam density increases down the tube.

In a triangular SW syneresis has a lesser effect on the equilibrium pressure, because the SW velocity and amplitude are attenuated by the foam. The separation of the points (Fig. 5) at fixed Z for an ℓ = 800 mm chamber implies that the density at a given distance from the foam surface decreases as the initial layer height increases.

In conclusion, we note that syneresis produces a nonuniform density distribution in a vertical foam column. At a column height h = 300 mm the density of bubbled foam near the surface is nearly three times higher than at the bottom. The density gradient reinforces extended-compression SWs and attenuates triangular SWs. Measurements of the relaxation times and equilibrium pressure serve to determine the structural changes occurring in the foam.

LITERATURE CITED

1. B. I. Palamarchuk, V. A. Vakhnenko, and A. V. Cherkashin, "Air shock waves in blast welding and cutting and their containment," Avtomat. Svarka, No. 2 (1988).
2. M. V. Kazakov, The Use of Surface-Active Materials in Fire Fighting [in Russian], Stroiizdat, Moscow (1977).
3. F. M. Gel'fand, Accident Prevention in Coal-Mine Blasting [in Russian], Nedra, Moscow (1974).
4. B. E. Gel'fand, A. V. Gubanov, and E. I. Timofeev, "The propagation of shock waves in foams," Fiz. Goreniya Vzryva, No. 4 (1981).
5. N. M. Kuznetsov, V. I. Timofeev, and A. V. Gubanov, "Analysis of shock wave propagation in thermodynamically stable foam," Fiz. Goreniya Vzryva, No. 5 (1986).
6. V. M. Kudinov, R. E. Gel'fand, A. V. Gubanov, and B. I. Palamarchuk, "Shock waves in foamy gas-liquid materials," Prikl. Mekh., 13, No. 3 (1977).
7. A. A. Borisov, B. E. Gelfand (Gel'fand), V. M. Kudinov, et al., "Shock waves in water foams," Acta Astron., 5, No. 4 (1978).
8. V. M. Kuidnov, B. I. Palamarchuk, V. A. Vakhnenko, et al., "Relaxation phenomena in a foamy structure," Progr. Astron. Aeron., 87, 96 (1983).
9. B. I. Palamarchuk and A. T. Malakhov, "Effect of relaxation processes on shock wave attenuation in aqueous foams," Proc. 4th Int. Symp. on Blast Processing of Materials, Gotval'dov (1979).
10. J. S. Krasinski (Krasinskii), A. Khosla, and V. Ramesh, "Dispersion of shock waves in liquid foams of high dryness fraction," Arch. Mech., 30, No. 4-5 (1978).
11. G. Patz and G. Smeets, "Pressure increase in two-phase media behind shock waves and by shock wave acceleration pistons," Proc. 15th Int. Symp. on Shock Tubes and Shock Waves, Berkeley, CA (1985).
12. P. M. Weaver and N. H. Pratt, "An experimental investigation of the mechanism of shock waves-aqueous foam interaction," Proc. 15th Int. Symp. on Shock Tubes and Shock Waves, Berkeley, CA (1985).
13. K. R. Kann, Capillary Hydrodynamics of Foams [in Russian], Nauka, Novosibirsk (1989).
14. A. F. Umnov, A. E. Golik, D. Yu. Paleev, and N. R. Shevtsov, Prevention and Containment of Underground Explosions [in Russian], Nedra, Moscow (1990).
15. J. Ikui, K. Matsuo, and Y. Yamamoto, "Fast-acting valves for use in short tubes," Bull. JSME, 20, No. 141 (1977).
16. F. L. Curzon and M. G. Phillips, "Low attenuation shock tube, driving mechanism and diaphragm characteristics," Canada, J. Phys., 49, No. 15 (1971).